

EFFECTS OF CHEMICAL KINETICS ON IGNITION OF HYDROGEN JETS

Bourgin, E,¹ Yang, C.,¹ Bauwens, L.,¹ and Fachini, F.F.²

¹University of Calgary, Calgary AB T2N 1N4, Canada, bauwens@ucalgary.ca

²Instituto Nacional de Pesquisas Espaciais, Cachoeira Paulista, SP 12630 Brazil, fachini@lcp.inpe.br

ABSTRACT

During the early phase of the transient process following a hydrogen leak into the atmosphere, a contact surface appears separating air heated by the leading shock from hydrogen cooled by expansion. Locally, the interface is approximately planar. Diffusion leads to a temperature decrease on the air side and an increase in the hydrogen-filled region, and mass diffusion, of hydrogen into air and of air into hydrogen, potentially resulting in ignition. This process was analyzed by Liñan and Crespo [1] for unity Lewis number and Liñan and Williams [2] for Lewis number less than unity. We included in the analysis the effect of a slow expansion [3, 4], leading to a slow drop in temperature, which occurs in transient jets. Chemistry being very temperature-sensitive, the reaction rate peaks close to the hot side of the interface, where only a small fuel concentration present close to the warm, air-rich side, which depends crucially upon the fuel Lewis number. For Lewis number unity, the fuel concentration due to diffusion is comparable to the rate of consumption by chemistry. If the Lewis number is less than unity, diffusion brings in more fuel than temperature-controlled chemistry consumes. For a Lewis number greater than unity, diffusion is not strong enough to bring in as much fuel as chemistry would burn; combustion is controlled by fuel diffusion. If the temperature drop due to expansion associated with the multidimensional jet does not lower significantly the reaction rate up to that point, analysis shows that ignition in the jet takes place. For fuel Lewis number greater than unity, chemistry does not lead to a defined explosion, so that eventually, expansion will affect the process; ignition does not take place [3, 4]. In the current paper, these results are extended to consider multistep chemical kinetics but for otherwise similar assumptions. High activation energy is no longer applicable. Instead, results are obtained in the short time limit, still as a perturbation superimposed to the self-similar solution to the chemically frozen diffusion solution. In that approximation, the initiation step, which consumes fuel and oxidant, is taken to be slow compared with steps that consume one of the reactants and an intermediate species. The formulation leads to a two point boundary value problem for set of coupled rate equations plus an energy equation for perturbations. These equations are linear, with variable coefficients. The coupled problem is solved numerically using a split algorithm in which chemical reaction is solved for frozen diffusion, while diffusion is solved for frozen chemistry. At each time step, the stiff coupled linear problem is solved exactly by projecting onto the eigenmodes of the stiff matrix, so that the solution is unaffected by stiffness. Since in the short time limit, temperature is only affected at the perturbation level, the matrix depends only on the similarity variable x/\sqrt{t} but it is otherwise time-independent. As a result, determination of the eigenvalues and eigenvectors is only done once (using Maple), for the entire range of discretized values of the similarity variable. The diffusion problem consists of a set of independent equations for each species. Each of these is solved using orthogonal decomposition onto Hermite polynomials for the homogeneous part, plus a particular solution proportional to time for the non-homogeneous (source) terms. That approach can be implemented for different kinetic schemes.

1. INTRODUCTION

The first comprehensive study of spontaneous ignition of hydrogen jets is due to Wolański & Wójcicki [7], although earlier anecdotal observations have been reported [8]. The relevance of jet ignition to hydrogen safety is clear [8], although there is a degree of ambiguity in that in some scenarios, ignition under the current mechanism will increase risks, while in other cases, early ignition may lower the risk of subsequent detonation.

Recent work, whether experimental [9, 10] or simulations [11, 12, 13], has been motivated by potential use of hydrogen as an energy carrier. Interplay between expansion due to shock multidimensionality, leading to a temperature drop [13], and preferential diffusion of hydrogen, carrying fuel in the high temperature region where air is mostly present, as the core explanation for the phenomenon, has been suggested by Rezaeyan et al. [3, 4].

Initially, the gas dynamics can be described as a shock tube (Riemann) problem, if in a one-dimensional geometry [9] (i.e., inside a tube), or its more complex multidimensional equivalent [14]. For chemistry to proceed, fuel and oxidant must be present, at a location where temperature is high enough to result in a significant reaction rate. Thus, if the controlling reaction step is characterized by an Arrhenius rate with high activation energy, ignition will occur close to the contact surface due to the shock tube problem, that separates hydrogen cooled by expansion from the high pressure source from air warmed by the leading shock.

In the near field, the initially nearly planar interface between hot air and cold hydrogen is affected by diffusion and advection due to flow, including instability. However, over the short time interval until ignition, the diffusion layer thickness remains small compared with its radius of curvature, instabilities may not have time to develop, and may not appear everywhere along the diffusion surface. Thus a one-dimensional model should remain realistic and meaningful. This is especially true if, as shown in a previous analysis, [3, 4] ignition requires the fuel to exhibit a low Lewis number, with a unity Lewis number being less favorable to ignition than a lower value. In that case, ignition should occur in regions along the diffusing interface that have not been affected by instabilities, since mixing due to instabilities or turbulent mixing will affect equally heat and fuel, in effect mimicking a unit Lewis number. In other words, instability or turbulence should hamper ignition rather than favor it.

The previous study [3, 4] was limited to single step kinetics, which arguably is not realistic. In the current study, an approach suitable to multistep kinetics is developed. Unfortunately the approach based upon high activation energy asymptotics does not lend itself readily to extension to multistep models. The approach still considers times short enough for the effects of chemistry to appear only as a perturbation to the flow and diffusion problem, in a frame of reference attached to the nearly planar diffusion layer. However the high activation energy assumption is replaced by assumptions on the magnitudes of different rates. Namely, three levels are identified, with initiation step(s) being much slower than most other rates, and termination being faster than most other rates, with both ratios comparable, and large. Time is scaled by the intermediate rate. Because initiation is slower, it only produces small concentrations of intermediate species. Thus only those steps in the kinetics that involve hydrogen or oxygen molecules, or a third body, and one of the radicals released by initiation are able to produce concentrations of intermediates at the same order. The termination step that is taken to be faster, however, features two intermediates with small concentration reacting, so that it produces water in a concentration of the same small order as all other intermediate species.

The related problem of ignition in a shear layer has been studied by Sánchez et al. [5] and Mellado et al. [6]. However these studies were limited to situations where temperatures were high enough so that the termination reaction under consideration here was unimportant.

2. PHYSICAL MODEL AND FROZEN FLOW SOLUTION

The formulation is as in [3, 4], except for chemical kinetics which assumes an arbitrary known multistep model, and the high activation energy assumption which is no longer made. It consists of conservation of mass, momentum and energy, including the effect of chemistry. Continuity is satisfied transparently using a mass-weighted spatial coordinate. Given that, in a nearly inertial frame of reference attached to the diffusion layer, the Mach numbers are small, momentum conservation results in pressure being approximately uniform spatially. Thus expansion is also spatially uniform, because the diffusive length is small compared with the length scales associated with the far field gas dynamics problem. Time is scaled such that, initially, there is little chemistry, the problem being then characterized by diffusion only: this is the so-called (chemically) frozen solution [1, 2]. To account for the small effect of chemistry, a perturbation is added to the frozen solution. Whether ignition takes place is determined by the trade off between the effect on temperature of heat release due to chemistry, and the temperature drop due to expansion.

Assuming diffusivities are inversely proportional to the square of density, a density-weighted spatial coordinate x is introduced, related to the original coordinate \hat{x} by

$$x = \frac{1}{\rho \sqrt{\alpha}} \int_0^{\hat{x}} \rho d\hat{x} \quad (1)$$

with α being the heat diffusivity. Then using a similarity variable $\eta = x/2\sqrt{t}$, and assuming time to be scaled by some t_0 such that the chemical reactions are negligible, the leading order formulation, called frozen flow by Liñan and Crespo [1] is reduced to diffusion of species and heat:

$$4t \frac{\partial y_k}{\partial t} - 2\eta \frac{\partial y_k}{\partial \eta} = \frac{1}{Le_k} \frac{\partial^2 y_k}{\partial \eta^2} \quad (2)$$

$$4t \frac{\partial T}{\partial t} - 2\eta \frac{\partial T}{\partial \eta} = \frac{\partial^2 T}{\partial \eta^2} + \frac{4t(\gamma - 1)T}{\gamma p} \frac{dp(t/t_0)}{dt} \quad (3)$$

where y_k is the mass fraction of species k , Le_k is the Lewis number for species k , T is temperature, p is a dimensionless pressure, and t_0 is the ratio of the time scale associated with expansion to the yet arbitrary time scale otherwise used. At $t = 0$, $p = 1$.

Boundary conditions are for $\eta \rightarrow -\infty$, $y_k \rightarrow 0$, except $y_F \rightarrow 1$, and $T \rightarrow T_F$. For $\eta \rightarrow \infty$ boundary conditions are $y_k \rightarrow 0$, except for $y_O \rightarrow 1$, and $T \rightarrow T_O$. The initial conditions match the boundary conditions, resulting in a self-similar solution, expressed using error functions

$$y_O = \frac{1 + \text{erf}(\eta \sqrt{Le_O})}{2}, \quad y_F = \frac{1 - \text{erf}(\eta \sqrt{Le_F})}{2}, \quad T = \left\{ T_O + \frac{(T_O - T_F)[\text{erf}(\eta) - 1]}{2} \right\} p^{(\gamma-1)/\gamma} \quad (4)$$

Mass fractions of intermediate reactants are zero in the frozen flow solution. Thus here, index k points only to O_2 and H_2 , with $y_k = 0$ for all other species.

Frozen flow results are shown in Fig. 1.

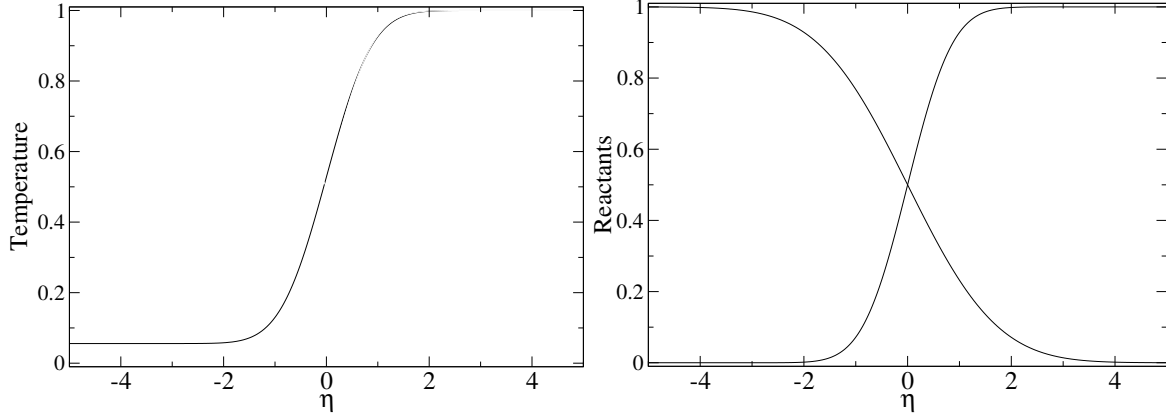


Figure 1: Left: Temperature as a function of η ; right: y_{O_2} (increasing from left to right) and y_{H_2} as functions of η .

3. CHEMICAL KINETICS AND THEIR EFFECT

Chemical kinetics adds source/sink terms in Eqs. (2,3) such that, before accounting for time scales, conservation of species k becomes

$$\frac{\partial y_k}{\partial t} - \frac{\eta}{2t} \frac{\partial y_k}{\partial \eta} - \frac{1}{4tLe_k} \frac{\partial^2 y_k}{\partial \eta^2} = \frac{1}{\rho} \sum \omega_{ijk} \quad (5)$$

The generic form of source ω_{ijk} is

$$\omega_{ik} = \pm C y_i^m y_j^n T^a \exp \frac{E}{RT} \quad (6)$$

in which constants C , m , n , a and E are specific to the reaction step under consideration. If the step in question consumes species k then ω_{ijk} is negative and $j = k$. If it produces species k then i and $j \neq k$. The value of these rates spans many orders of magnitudes, resulting in a wide range of scales, and also the issue of stiffness in numerical simulation of chemical kinetics. For instance, for the variant of the San Diego scheme mentioned in Boivin et al. [15], initiation, due to step 6 reverse (see [15], Table 1, step 6r), is characterized by a rate of $1.94 \times 10^9 s^{-1}$ on the hot air side of the interface, assuming an initial pressure in the hydrogen vessel of 50 MPa. Most other rates are in around $10^{12} s^{-1}$, except for 8 forward, which is $5.23 \times 10^{15} s^{-1}$. The latter step is the only one producing significant amounts of water hence being exothermic.

Thus, If time is scaled by one of the rates of around $10^{12} s^{-1}$ (the reference rate), calling ϵ the ratio between the rate of 6 reverse and the reference rate, then while in the diffusion layer, y_{O_2} , y_{H_2} are order unity, reaction 6r produces y_{HO_2} and y_H of order ϵ . Then, at order ϵ , 1f produces y_H and y_{OH} , 2f produces y_{OH} and y_H , 3f, y_{H_2O} and y_H , 4f, y_{HO_2} , y_{HO_2} and y_{OH} , 8r, y_H and y_{OH} , 9r, y_H , 10r, y_{HO_2} , 11f, $y_{H_2O_2}$ and finally, 12f, y_{OH} . However, 5f, 5r, 6f, 7, 10f, 11r and 12r only contribute at order ϵ^2 , and, because its rate is higher by order $1/\epsilon$, 8f produces water at order ϵ .

Thus, while H_2 and O_2 are present at leading order, HO_2 , H , OH , O , H_2O_2 and water are present at order ϵ only. These are the intermediate species that need being accounted for at order ϵ . At leading

order, rates are constant in times but they vary with η . The six perturbation equations are of the form:

$$\frac{\partial y_k^{(1)}}{\partial t} - \frac{\eta}{2t} \frac{\partial y_k^{(1)}}{\partial \eta} - \frac{1}{4Le_k t} \frac{\partial^2 y_k^{(1)}}{\partial \eta^2} = \frac{1}{\rho} \sum_i a_{ik} y_i^{(1)} + \frac{s}{\rho} + \frac{b}{\rho} y_H^{(1)} y_{OH}^{(1)} \quad (7)$$

in which subscript (1) points to perturbation of order ϵ , index i and k refer to intermediate species, with rates $a_{ik}(\eta) = k_{ik} y_k^{(0)}$ corresponding to the effect of reactions involving one intermediate species and either H_2 or O_2 , and $b(\eta)$ corresponding to termination. The latter term, due to 8f, is present only in the equations for H , OH and H_2O . Source $s_k(\eta)$, due to initiation, 6r, is present only for HO_2 and H .

The effect of the third body (M) on rates is computed as in Ref. [16].

Coefficients a_{ik} , b , and ρ depend upon leading order temperature and concentrations in H_2 and O_2 , i.e. upon the frozen solution, hence the dependence on η . The resulting problem is nonlinear because of the last term. The equations are coupled through the first and last term on the r.h.s. It requires a numerical solution.

4. NUMERICAL SOLUTION

A numerical solution is constructed by splitting, at each time step, the solutions of

$$\frac{\partial y_k^{(1)}}{\partial t} - \frac{\eta}{2t} \frac{\partial y_k^{(1)}}{\partial \eta} - \frac{1}{4Le_k t} \frac{\partial^2 y_k^{(1)}}{\partial \eta^2} = \frac{s}{\rho} \quad (8)$$

$$\frac{\partial y_k^{(1)}}{\partial t} = \frac{1}{\rho} \sum_i a_{ik} y_i^{(1)} \quad (9)$$

$$\frac{\partial y_k^{(1)}}{\partial t} = \frac{1}{\rho} \frac{b}{\rho} y_H^{(1)} y_{OH}^{(1)} \quad (10)$$

The first equation is decoupled, i.e. the equation for each species k is solved independently of all others. The second equation is fully coupled and potentially stiff.

The third equation only involves H and OH but appears as a source in H_2O , and it also is potentially stiff. Because it involves only two species, a second order accurate absolutely stable predictor-corrector integration scheme based upon backward integration only involves solutions of quadratic algebraic equations, hence requiring no iteration.

As to the second equation, the matrix of the coefficients, $A = a_{ik}$ depends upon η but not time. Thus eigenmodes and eigenvectors can be computed once and for all for a range of discretized values of η . Stiffness is then dealt with by projecting onto eigenmodes, advancing in time on the separated eigenvectors, and reconstructing the solution at the new time step.

A similar finite differences approach might seem natural also for the six decoupled Eqs. (8). However a stability analysis shows that for large positive or negative values of η , typical schemes become unstable.

In the absence of the effect of the other two split equations, and given that the initial values of y at $t = 0$ are $y = 0$, its solution would be of the form $y = tY(\eta)$. More generally, its solution can be constructed as a particular solution, still of the form $y = tY(\eta)$, plus a solution of the homogeneous equation, with, at each time step, initial solution based upon the solution before the time step, minus the particular solution at that time. It turns out that the solution to the homogeneous equation can be expressed as a series solution based upon Hermite polynomials.

Finding $Y(\eta)$ requires solving a two point boundary value problem:

$$Y - \frac{\eta}{2} \frac{dY}{d\eta} - \frac{1}{4Le} \frac{d^2Y}{d\eta^2} = \frac{s}{\rho} \quad (11)$$

with zero boundary conditions at infinity. Because error functions approach constant values very quickly at infinity, s becomes extremely small for still moderate values of η , so that an integration domain from -20 to $+20$ is more than enough. A numerical solution is obtained iteratively, guessing the coefficient of an approximation to the solution for large η , using a secant method. For large η , $s \rightarrow 0$ and the solution approaches

$$Y = C\eta^{-2} \exp -Le\eta^2, \quad \frac{dY}{d\eta} = C(-3\eta^{-4} - 2Le\eta^{-2}) \exp -Le\eta^2 \quad (12)$$

As to the homogeneous equation, of the form

$$\frac{\partial Y}{\partial t} - \frac{\eta}{2t} \frac{\partial Y}{\partial \eta} - \frac{1}{4Let} \frac{\partial^2 Y}{\partial \eta^2} = 0 \quad (13)$$

writing $Y = f(t)z(\eta)$, one finds

$$\frac{t}{f} \frac{df}{dt} = \frac{\eta}{2z} \frac{dz}{d\eta} + \frac{1}{4Lezt} \frac{d^2z}{d\eta^2} = \sigma \quad (14)$$

The eigenvalue problem

$$\frac{d^2z}{d\eta^2} + 2Le\eta \frac{dz}{d\eta} - 4Le\sigma z = 0 \quad (15)$$

with zero boundary conditions has eigenvalues $\sigma_n = -(n+1)/2$ with $n = 0, 1, 2, \dots$. The corresponding eigensolutions are

$$z_n = \exp(-Lez^2) H_n(z \sqrt{Le}) \quad (16)$$

in which H_n is the n^{th} Hermite polynomial. The eigensolution are orthogonal under the following dot product:

$$\int_{-\infty}^{\infty} e^{-Le\eta^2} H_m(\eta \sqrt{Le}) H_n(\eta \sqrt{Le}) d\eta = 0 \text{ for } m \neq n \quad (17)$$

while

$$\int_{-\infty}^{\infty} e^{-Le\eta^2} H_m^2(\eta \sqrt{Le}) d\eta = \frac{2^m \sqrt{\pi n!}}{\sqrt{Le}} \quad (18)$$

Thus the solution can be written as

$$z = \sum_{n=0}^{\infty} C_n t^{-(n+1)/2} z_n \quad (19)$$

The coefficients C_n at the beginning t_i of the time step are obtained from the integrals above as

$$\int_{-\infty}^{\infty} H_m(\eta \sqrt{Le}) Y d\eta = C_m t_i^{\sigma_m} \frac{2^m \sqrt{\pi n!}}{\sqrt{Le}} \quad (20)$$

Next, the solution is reconstructed at t_{i+1} using Eq. (19).

A difficulty appears, however, for large absolute values of η , when rates become very small, while $H_2(\eta)$ becomes very large. In the true solution, rates become small faster than H_2 becomes large, so that the approach is fundamentally sound, but numerical errors associated with the other steps in the solution are limited by numerical accuracy, leading to non-convergence of the analysis and reconstruction process. The workaround is then to zero the results of the other two steps outside of the range of interest. One verifies that the approach is correct: rebuilding the profiles at t_i yields the correct profiles. The issue appears to be associated with the problem itself rather than the technique; this is likely why finite differences schemes become unstable for large η .

As to implementation, evaluation of the eigenvalues and eigenvectors of matrix $A(\eta)$ was performed using Maple. Results were read into the code dealing with solving the global problem. An interval from $\eta = -20$ to $+20$ was used. A good representation of the solution required using 500 to 1000 modes in the Hermite series.

Table 1: Kinetics - Rates of form $AT^n \exp(-E/RT)$

No. [15]	Step	A_f	n_f	E_f	A_r	n_r	E_r
1	$\text{H} + \text{O}_2 \rightarrow \text{OH} + \text{O}$	3.52×10^{16}	-0.70	71.42			
2	$\text{H}_2 + \text{O} \rightarrow \text{OH} + \text{H}$	5.06×10^{16}	2.67	26.32			
3	$\text{H}_2 + \text{OH} \rightarrow \text{H}_2\text{O} + \text{H}$	1.17×10^9	1.30	15.21			
4	$\text{H} + \text{O}_2 + \text{M} \rightarrow \text{HO}_2 + \text{M}$	4.65×10^{12}	0.44	0.0			
6	$\text{HO}_2 + \text{H} \leftarrow \text{H}_2 + \text{O}_2$				2.69×10^{12}	0.36	231.9
8	$\text{H} + \text{OH} + \text{M} \rightleftharpoons \text{H}_2\text{O} + \text{M}$	4.0×10^{22}	-2.0	0.0	1.03×10^{23}	-1.75	494.1
11	$\text{HO}_2 + \text{H}_2 \rightarrow \text{H}_2\text{O}_2 + \text{H}$	1.62×10^{11}	0.61	100.1			
12	$\text{H}_2\text{O}_2 + \text{M} \rightarrow 2\text{OH} + \text{M}$	2.62×10^{19}	-1.39	214.7			

5. RESULTS AND DISCUSSION

Results were obtained, based upon the kinetic scheme already mentioned [15], for a pressure ratio of 500. Under the scaling assumptions above, the kinetic scheme is reduced to the steps shown in Table 1.

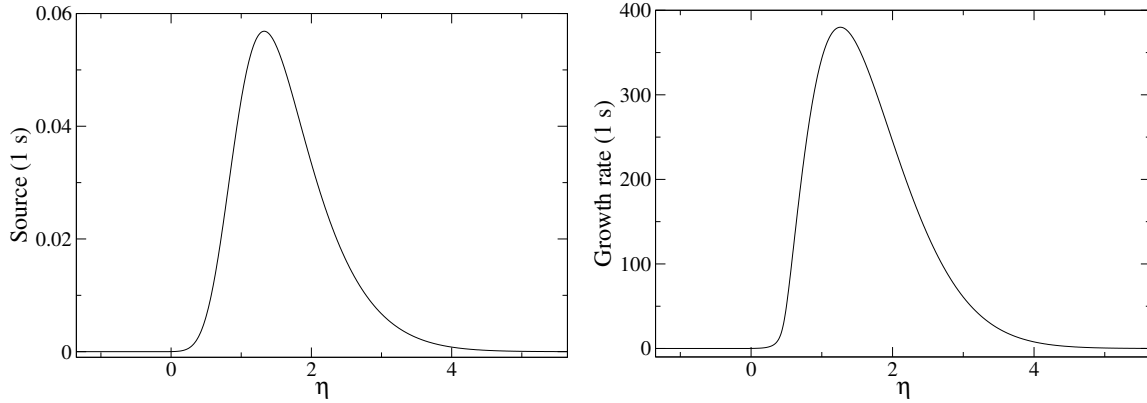


Figure 2: Left: source term s due to initiation as a function of η ; right: Positive eigenvalue of A as a function of η .

Figure 2 shows how the source and the single positive eigenvalue of matrix A vary with η . These results show that initiation occurs well into the warm air region, where chain-branching also appears to be most effective well into the cold hydrogen region. It is worth noting that in the scheme that was used [15], for step 4, two rates are given, respectively for low and high pressure. The former depends on temperature through a temperature exponent equal to -1.4 while the latter, which was used in the current results, is positive, equal to 0.44 . Based upon results by Troe, Konnov [17] also proposes an exponent of $+0.44$.

Figure 3 shows evolution of species during early times when initiation dominates, while Fig. 4 shows the same results at transition times, and Fig. 5 shows them at times late enough that initiation is no longer important.

First, from Fig. 3, initially, initiation results in an approximately linear growth of y_H and y_{HO_2} (not shown), mainly around $\eta = 1.3$. Linear growth is consistent with the role of the source terms, which enter the numerical solution through Eq. (8), with initial behavior $tY(\eta)$. As to y_O and y_{H_2O} , their initial peak, centered around $\eta = 0.8$, is much smaller than the peak in the species released by initiation. That location is not located at the value of η at which chain-branching, characterized by the positive eigenmode, peaks, which, according to Fig. (2), is further right. Since these intermediate species, and water, are initially absent, their initial growth should be faster than exponential; however the jumps between values for the upper curves look more like proportional to time. Peaks in y_O and y_{H_2O} have values very close to each other. As to y_{OH} , its value remains quite small. It appears that consumption associated with reaction no. 8, which is very strong, is dominated by supply of OH, so that at least initially, y_{OH} rapidly reaches a steady state with value very close to zero. Likewise, $y_{H_2O_2}$ remains consistently small, and as a result, HO_2 , the second species produced by initiation, plays no significant role either.

As time increases, according to Fig. 4, the behavior changes. More and more water appears, and eventually, slightly later than 2 seconds into the process, its concentration becomes larger than y_H ; y_O continues increasing, but at a slower pace. Water concentration at its peak now exhibit faster growth than the species released by initiation.

At later times, as Fig. 5, water concentration, continues growing rapidly, and becomes large, especially when compared with the initiation peak, which only grows linearly. The peak in water concentration shifts slightly toward the right. This is because a shift occurs between O and OH as the critical reactant. Indeed, the peak in y_O is shifting to the right. In the region around $\eta = 0.5$, its value is actually diminishing, as step 8 now consumes more O than is produced so the O inventory drops. Later on, in that region, results (not shown) indicate that y_O reaches a near-zero steady state and becomes the

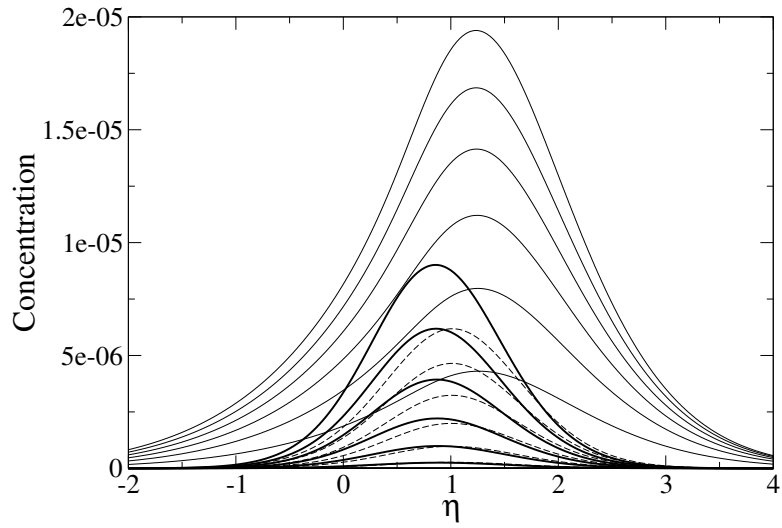


Figure 3: Time from 0.2 to 2.0 ms. y_H (thin continuous line), y_{H_2O} (thick) and y_O (interrupted line) as functions of η .

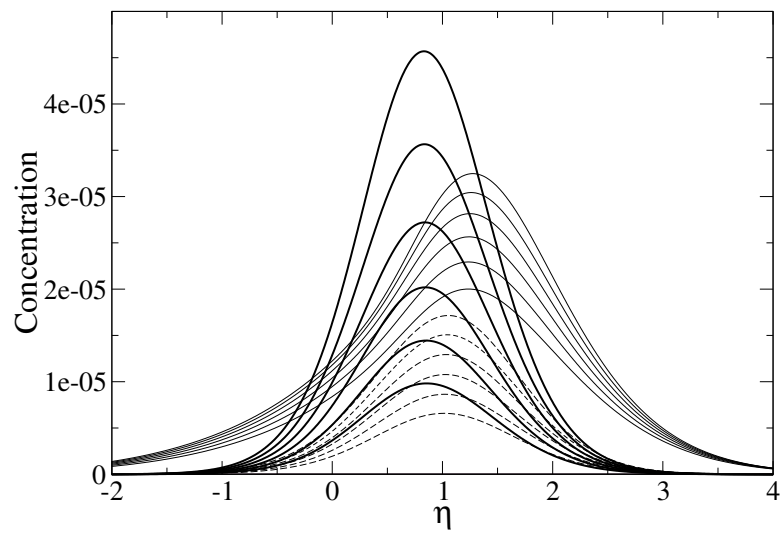


Figure 4: Time from 1.25 to 2.5 ms. y_H (thin continuous line), y_{H_2O} (thick) and y_O (interrupted line) as functions of η .

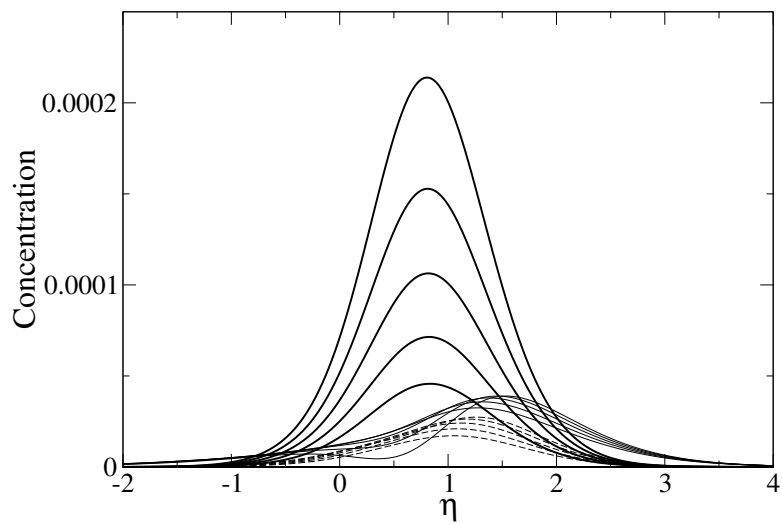


Figure 5: Time from 2.5 to 4.5 ms. y_H (thin continuous line), y_{H_2O} (thick) and y_O (interrupted line) as functions of η .

limiting reactant, while y_{OH} starts increasing. This shifts the peak in water production toward higher temperatures.

As the perturbation values become large, the assumption that temperature changes have negligible effects will no longer be valid, and results from the current model are no longer realistic, particularly for the rates with high activation energy.

Although no results on the effect of ignition on temperature are currently available, the termination step, which releases water, is strongly exothermic so that temperature increase is strongly correlated with water production. Ultimately, a quantitative cutoff between ignition/no ignition will be obtained by comparing the temperature increase due to chemistry and the temperature decrease due to expansion. If and only if the latter is stronger, ignition will take place.

Previous analysis [3, 4] pointed out the crucial role of the small Lewis number of hydrogen in jet ignition. In the current results, the hydrogen Lewis number still plays a key role, in the initiation process. Indeed, initiation occurs around $\eta = 1$, well within the hot air region, and the production of radicals is proportional to the fuel concentration. Because in the current model, activation energies play no role, the clear cutoff that was obtained in the previous analysis is of course no longer present. Still, for fuels with a larger Lewis number, as pointed out in [4], initiation will easily be slower by a factor 10 to 15.

The radical H produced by initiation, which plays a key role in subsequent processes, is characterized by an even smaller Lewis number. The combined effect of the two Lewis numbers should thus slow down the ignition process by a factor close to 100, making it much more susceptible to expansion. As in the previous study for single step kinetic [3, 4], initial incipient reaction occurs well within the hot air region where little hydrogen is present. However, because hydrogen exhibits a mass diffusion larger than heat diffusion, i.e. a small Lewis number, much more hydrogen is brought in by diffusion than would be the case with high Lewis number fuels such as hydrocarbons. The previous conclusion [3, 4] is thus confirmed whereby the experimental observation that only hydrogen is susceptible of jet ignition is a Lewis number effect.

6. CONCLUSION

An analysis was performed of diffusion ignition at the diffusing interface between cold hydrogen and hot air, in an environment where spatially uniform pressure is slowly decreasing. Assumptions on rate magnitude were proposed which are reasonably realistic, yet allow to distinguish between three ranges, associated respectively with initiation, which is slow, termination, which is fast, and other steps with intermediate rate values. These assumptions can be adapted to arbitrary complex schemes.

The analysis resulted in a problem combining reaction and diffusion that required numerical solution. An algorithm was developed based upon a split algorithm. Diffusion was solved by projection onto Hermite polynomials, which provided a set of orthogonal base functions. To avoid stiffness issues, the linear part of the kinetics was solved by projecting into eigenmodes of the Jacobian matrix at each time step. As to the nonlinear part, namely step 8, its solution at each time step was based upon the exact solution for frozen diffusion and frozen linear kinetics.

Results were presented for a variant of the San Diego scheme [15]. However, most of the crucial steps in the current study appear to be characterized by similar rate expressions in other schemes, except possibly for initiation, so that results are not expected to be significantly different for other kinetic schemes.

Results confirm the important role of the Lewis number in jet ignition that emerged from a previous

analysis [3, 4]. This is because initiation, which is slow and stiff, occurs well within the warm air region. Hydrogen, which, in contrast with typical fuels, diffuses much more effectively than heat, penetrates much more easily into the warm region where initiation takes place.

ACKNOWLEDGMENTS

Research supported by the NSERC Hydrogen Canada (H2CAN) Strategic Research Network, and by the NSERC Discovery Grants program.

REFERENCES

1. Liñán, A. and Crespo, A., An Asymptotic Analysis of Unsteady Diffusion Flames for Large Activation Energies, *Combustion Science and Technology*, **14**, 1976, pp. 95-117.
2. Liñán, A. and Williams, F.A., Ignition in an Unsteady Mixing Layer Subject to Strain and Variable Pressure, *Combustion and Flame*, **95**, 1993, pp. 31-46.
3. Rezaeyan, N., Bauwens, L., Radulescu, M. and Fachini, F.F., Influence of Lewis Number and Expansion on Jet Ignition, 24th International Colloquium on the Dynamics of Explosions and Reactive Systems, Irvine, CA, Aug. 2011.
4. Rezaeyan, N., Bauwens, L., Radulescu, M. and Fachini, F.F., The Crucial Role of the Lewis Number in Jet Ignition, 4th International Conference on Hydrogen Safety, San Francisco, CA, Sept. 2011.
5. Sánchez, A.L., Liñán, A. and Williams, F.A., A WKB analysis of radical growth in the hydrogen-air mixing layer, *Journal of Engineering Mathematics*, **31**, 1997, pp. 119130.
6. Mellado, J.D., Sánchez, A.L., Kim, J.S. and Liñán, A. Branched-chain ignition in strained mixing layers, *Combustion Theory and Modelling*, **4**, 2000, pp. 265288.
7. Wolański, P. and Wójcicki, S., Investigation into the Mechanism of the Diffusion Ignition of a Combustible Gas Flowing into an Oxidizing Atmosphere, *Proceedings of the Combustion Institute*, **14**, 1973, pp. 1217-1223.
8. Astbury, G. R. and Hawksworth S.J., Spontaneous Ignition of Hydrogen Leaks: A Review of Postulated Mechanisms, *International Journal of Hydrogen Energy*, **32**, 2007, pp. 2178-2185.
9. Dryer, F.L., Chaos, M., Zhao, Z., Stein, J.N., Alpert, J.Y. and Homer, C.J., Spontaneous Ignition of Pressurized Release of Hydrogen and Natural Gas into Air, *Combustion Science and Technology*, **179**, 2007, pp. 663-694.
10. Oleszczak, P. and Wolański, P., Ignition during Hydrogen Release from High Pressure into the Atmosphere, *Shock Waves*, **20**, 2010, pp. 539-550.
11. Liu, Y.F., Tsuboi, N., Sato, H., Higashino, F. and Hayashi, A. K., Numerical Analysis of Auto-ignition in High Pressure Hydrogen Jetting into Air, *Proceedings of the Combustion Institute*, **31**, 2007, pp. 1217-1225.
12. Xu, B. P., Hima, L.E.L., Wen, J.X. and Tam, V.H.Y., Numerical Study of Spontaneous Ignition of Pressurized Hydrogen Release into Air, *International Journal of Hydrogen Energy*, **34**, 2009, pp. 5954-5960.
13. Maxwell, B. M. and Radulescu, M.I., Ignition Limits of Rapidly Expanding Diffusion Layers: Application to Unsteady Hydrogen Jets, *Combustion and Flame*, doi:10.1016/j.combustflame.2011.03.001.
14. Radulescu, M. I. and Law, C.K., The Transient Start of Supersonic Jets, *Journal of Fluid Mechanics*, **578**, 2007, pp. 331-369.
15. Boivin P., Jimenez C., Sánchez A.L., and Williams F.A., An explicit reduced mechanism for H₂ -air combustion, *Proceedings of the Combustion Institute*, **33**, 2011, pp. 517523.
16. Seshadri, K., Peters, N. and Williams, F.A., Asymptotic analyses of stoichiometric and lean hydrogen-air flames, *Combustion and Flame*, **96**, 1994, pp. 407-427.
17. Konnov, A., Remaining uncertainties in the kinetic mechanism of hydrogen combustion, *Combustion and Flame*, **152**, 2008, pp. 507-528.